Pertanika J. Sci. & Technol. 24 (1): 53 - 70 (2016)

SCIENCE & TECHNOLOGY

Journal homepage: http://www.pertanika.upm.edu.my/

Scaling Group Transformation for MHD Double-Diffusive Flow Past a Stretching Sheet with Variable Transport Properties Taking into Account Velocity Slip and Thermal Slip Boundary Conditions

Uddin, M. J.[1, 3], Khan, W. A.[2*] and Ismail, A. I. M.[3]

[1]*Department of Mathematics, American International University-Bangladesh, Banani, Dhaka 1213, Bangladesh*

[2]*Department of Engineering Sciences, PN Engineering College, National University of Science and Technology, Karachi 75350, Pakistan*

[3]*School of Mathematical Sciences, Universiti Sains Malaysia, Penang 11800, Malaysia*

ABSTRACT

The steady two-dimensional laminar mixed convective boundary layer flow of a viscous incompressible electrically conducting Newtonian fluid along a moving stretching sheet embedded in a porous medium was studied numerically. We used temperature dependent viscosity and thermal conductivity and concentration dependent mass diffusvity. Further, the velocity and thermal slip boundary conditions were applied at the surface of the sheet. The governing transport equations were reduced to similarity equations using scaling group of transformation, before being sloved numerically by using the fourth-fifth order Runge-Kutta-Fehlberg method from Maple 13. Our analysis revealed that the mass diffusivity parameter causes both temperature and concentration to increase whilst thermal conductivity parameter increases the temperature. It was also revealed that the rate of heat and mass transfer increased with the increasing of velocity slip, viscosity and power law parameters. Comparisons with previous published works are reported and good agreements were found.

Keywords: Variable transport properties, double-diffusion, Lie group, velocity and thermal slip, MHD

INTRODUCTION

Momentum, heat and mass transfer in porous media have applications in the petroleum industry, geothermal processes, control of pollutant spread in ground water, heat exchange between soil and atmosphere, flat plate solar collectors, solar power collectors, food industries, insulation of nuclear reactors, nuclear waste management and many other areas (Nield & Bejan, 2013). Transport

Article history:
Received: 6 June 2013
Accepted: 22 September 2015

E-mail addresses:
Uddin, M. J. (jashim_74@yahoo.com), wkhan_2000@yahoo.com (Khan, W. A.), izani@cs.usm.my (Ismail, A. I. M.)
*Corresponding author

ISSN: 0128-7680

phenomenon due to motion of a stretching sheet has attracted the interest of researchers because of its diverse engineering applications such as the aerodynamic extrusion of plastic sheets, the boundary layer along a liquid film in condensation process and the cooling of the metal plate in a cooling bath as well as its use in the glass and fibre industries (Vajravelu *et al*., 2011). Fluid flow over a linearly stretching surface was first analysed by Crane (1970). This problem was widely studied for natural/combined convective steady/unsteady flow over various geometries for both Newtonian and non-Newtonian fluid in clear/porous media. A few investigations are presented in the paper by Ishak *et al*. (2009) and Abdel-Rahman (2010). Thermal radiation effect plays an important role in controlling heat transfer in the industry where the quality of the final products depends on heat controlling factors to some extent. High temperature plasmas, cooling of nuclear reactors, liquid metal fluids and power generation systems are some important applications of radiative heat transfer from a surface plate to conductive fluids.

Heat flux caused by a concentration gradient is known as diffusion-thermo effect (Dufour effect) whilst species differentiation owing to the gradient of temperature is known as thermal-diffusion effect (Soret effect) (Eckert & Drake, 1972). It is known that these effecst are smaller than the effects described by Fourier and Fick's laws, but there are many practical applications in which their effects are significant. For example, the Soret effect has been used for isotope separation and in the mixing between gasses with very light molecular weight and of medium molecular weight (Hayat *et al*., 2010). The effect of Soret number and Dufour number on MHD free convective heat and mass transfer over a vertical stretching surface in a porous medium was studied by Mansour *et al*. (2008). The steady stagnation point flow over a vertical stretching surface in the presence of species concentration and mass diffusion under the Soret and Dufour effects was studied by Tsai and Huang (2009). Postelnicu (2010) describes Dufour and Soret effects on two-dimensional stagnation point flow in a saturated porous medium.

The above literature review revealed that the previous analyses are concerned with the boundary layer flow and heat and mass transfer in a Newtonian fluid using a conventional no-slip boundary conditions. However, fluid flow in micro/nanoscale such as micropumps, microtubines, micro heat exchangers, sensors and actuators are important for micro- and nanoscience and the conventional no slip boundary condition at the solid–fluid interface must be replaced with the slip condition (Jiji, 2010). Slip flows occur in a variety of technological applications, for example, extrusion dies (Gifford 2004), foam production (Ireland & Jameson, 2009), fabrication, the design of microelectromechanical systems (Lahjomri & Oubarra, 2013) and fluidic cells in medicine (Khaled & Vafai, 2004), in which increasing wall slip has been shown to generate enhanced cooling and flow fluctuations. Slip effect on flow field has been studied by various authors: Aziz (2010), Uddin *et al*. (2012) and Noghrehabadi *et al*. (2012). All of these researchers restricted their investigation to constant transport properties. However, they are not constants. No study, as far as these authors are aware, has been reported in the literature for the investigations of MHD mixed convective flow past a stretching sheet with slip boundary conditions and variable transport properties.

The aim of this study was to extend the work of Abdel Rahman (2010) to include the effect of velocity and thermal slip as well as temperature dependent thermal conductivity and concentration dependent mass diffusivity. The transport equations were reduced to similarity equations using similarity variables obtained by a scaling group analysis and then

solved numerically. The effect of the key physical parameters on the dimensionless velocity, temperature, concentration, skin friction, rate of heat transfer and the rate of mass transfer were examined and discussed. The problem reported in this paper has not been investigated in the literature despite its applications in many engineering processes, such as nuclear waste, polymer production, dispersion of chemical pollutants through water-saturated soil, geothermal energy extractions, plasma studies, liquid metal fluids, power generation systems, molecular dynamics and micro/nanofluidics.

FORMULATION OF THE BASIC TRANSPORT EQUATIONS

A steady two-dimensional magnetohydrodynamic (MHD) double-diffusive combined convective laminar incompressible Newtonian fluid flow in a Darcian porous medium along a moving vertical stretching surface was considered. The flow model and coordinate system is shown in Fig.1.

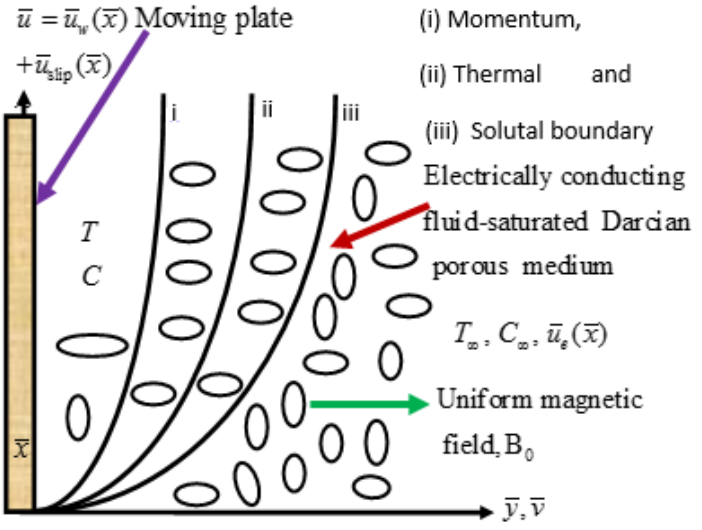

Fig.1: Uptake mechanism of thymidine and ^{18}F-FLT.

A magnetic field of uniform strength B_0 was applied perpendicular to the plate. We ignored induced magnetic fields and hence ingored the magnetic Reynolds number. It was assumed that a first-order homogenous isothermal irreversible chemical reaction would take place between the chemical constitute of the plate and the ambient fluid. The Boussinesq approximation was taken into account. Following Seddeek and Salem (2005), we assumed the temperature dependent viscosity would vary according to $\mu(T) = \mu_\infty e^{-\alpha_0 \theta}$, where μ_∞ is the constant viscosity far away from the plate and α_0 is the viscosity parameter depending on the nature of the fluid, Θ is the dimensionless temperature defined in Eqn. (6). It was further assumed that the temperature dependent thermal conductivity varied linearly as $k(T) = k_\infty [1 + c_1 (T - T_\infty)] = k_\infty [1 + A\theta]$, where k_∞ is the constant undisturbed thermal conductivity far away from the plate, c_1 is a

constant which depends on the fluid and $A = c_1 \Delta T$ is the thermal conductivity parameter. We further assumed that mass diffusivity varied linearly as where D_∞ is the constant concentration diffusivity far away from the plate and $Dc = c_2 \Delta C$ is a concentration diffusivity parameter (White & Subramanian, 2010), ϕ is the dimensionless concentration defined in Eqn. (6). Here c_2 is a constant. The boundary layer equations in dimensional form are (Abdel-Rahman, 2010):

$$\frac{\partial \bar{u}}{\partial \bar{x}} + \frac{\partial \bar{v}}{\partial \bar{y}} = 0, \tag{1}$$

$$\bar{u}\frac{\partial \bar{u}}{\partial \bar{x}} + \bar{v}\frac{\partial \bar{u}}{\partial \bar{y}} = \nu_\infty \frac{\partial}{\partial \bar{y}}\left(e^{-\alpha_0 \theta}\frac{\partial \bar{u}}{\partial \bar{y}}\right) + \bar{u}_e \frac{d\bar{u}_e}{d\bar{x}} - \frac{\nu_\infty}{k}(\bar{u} - \bar{u}_e) - \frac{\sigma B_0^2}{\rho}(\bar{u} - \bar{u}_e) \tag{2}$$
$$+ g\beta_T (T - T_\infty) + g\beta_C (C - C_\infty),$$

$$\bar{u}\frac{\partial T}{\partial \bar{x}} + \bar{v}\frac{\partial T}{\partial \bar{y}} = k_\infty \frac{\partial}{\partial \bar{y}}\left[(1 + A\theta)\frac{\partial T}{\partial \bar{y}}\right] + \frac{16\sigma_1 T_\infty^3}{3\rho_\infty c_p k_1}\frac{\partial^2 T}{\partial \bar{y}^2} + \frac{Q_0}{\rho_\infty c_p}(T - T_\infty) \tag{3}$$
$$+ \frac{k_T D_m}{c_s c_p}\frac{\partial}{\partial \bar{y}}\left[(1 + Dc\phi)\frac{\partial C}{\partial \bar{y}}\right],$$

$$\bar{u}\frac{\partial C}{\partial \bar{x}} + \bar{v}\frac{\partial C}{\partial \bar{y}} = D_\infty \frac{\partial}{\partial \bar{y}}\left[(1 + Dc\phi)\frac{\partial C}{\partial \bar{y}}\right] - k_0 (C - C_\infty) \tag{4}$$
$$+ \frac{K_T D_\infty}{T_m}(1 + Dc\phi)\frac{\partial^2 T}{\partial \bar{y}^2}.$$

The relevant boundary conditions are (Jiji, 2010):

$$\bar{u} = c\bar{x} + N_1 \nu_\infty \frac{\partial \bar{u}}{\partial \bar{y}},\ \bar{v} = 0,\ T = T_w(\bar{x}) + D_1 \frac{\partial T}{\partial \bar{y}}, C = C_w(\bar{x}) \text{ at } \quad \bar{y} = 0, \tag{5}$$
$$\bar{u} \to \bar{u}_e(\bar{x}) = a_1 \bar{x},\ \ T \to T_\infty,\ \ C \to C_\infty \quad \text{as} \quad \bar{y} \to \infty.$$

Here $(\bar{u}, \bar{v})$: Darcian velocity components along the $\bar{x}$ and $\bar{y}$ -axes, $\mu(T)$: temperature dependent viscosity, ρ_∞: density of the ambient fluid, ν_∞ constant kinematic viscosity, $\bar{u}$ free stream velocity, K_0: permeability of the porous media, σ: electric conductivity, g: acceleration due to gravity, β_T: volumetric coefficient of thermal expansion, β_c: volumetric coefficient of mass expansion, C_p: specific heat at constant pressure, $k(T)$: temperature dependent thermal conductivity, Q_0: heat generation/absorption constant, k_T: thermal diffusion ratio, C_s: concentration susceptibility, $D(C)$: concentration dependent mass diffusivity, T_m: mean fluid temperature, k_0: reaction rate constant, N_1: velocity slip factor and D_1: thermal slip factor. Also, c and a_1 are the positive constant σ_1 : Stefan-Boltzmann constant, while k_1: Rosseland means absorption coefficient.

Using the following are dimensionless variables:

$$x=\frac{\overline{x}}{\sqrt{\nu_\infty / c}},\ y=\frac{\overline{y}}{\sqrt{\nu_\infty / c}},\ u=\frac{\overline{u}}{\sqrt{c\nu_\infty}},\ v=\frac{\overline{v}}{\sqrt{c\nu_\infty}},\ u_e=\frac{\overline{u}_e}{\sqrt{c\nu_\infty}},$$
$$\theta=\frac{T-T_\infty}{\Delta T},\phi=\frac{C-C_\infty}{\Delta C},\Delta T=T_w-T_\infty,\Delta C=C_w-C_\infty. \tag{6}$$

and hence, using the stream function Ψ defined by $u=\frac{\partial\psi}{\partial y},\ v=-\frac{\partial\psi}{\partial x},$ we have from Eqns. (2)-(4):

$$\Delta_1\equiv\frac{\partial\psi}{\partial y}\frac{\partial^2\psi}{\partial x\partial y}-\frac{\partial\psi}{\partial x}\frac{\partial^2\psi}{\partial y^2}+\alpha_0\,e^{-\alpha_0\theta}\frac{\partial\theta}{\partial y}\frac{\partial^2\psi}{\partial y^2}-e^{-\alpha_0\theta}\frac{\partial^3\psi}{\partial y^3}$$
$$-u_e\frac{du_e}{dx}+(\Omega+M)\left(\frac{\partial\psi}{\partial y}-u_e\right)-\frac{g\,\beta_T\,\Delta T}{c\sqrt{c\nu_\infty}}\theta-\frac{g\,\beta_C\,\Delta C}{c\sqrt{c\nu_\infty}}\phi=0, \tag{7}$$

$$\Delta_2\equiv\frac{\partial\psi}{\partial y}\frac{\partial\theta}{\partial x}-\frac{\partial\psi}{\partial x}\frac{\partial\theta}{\partial y}+\frac{\partial\psi}{\partial y}\theta\frac{\partial}{\partial x}[\ln(\Delta T)]-\frac{1}{\mathrm{Pr}}\left[\frac{R+1+A\theta}{R}\right]\frac{\partial^2\theta}{\partial y^2}$$
$$-\frac{1}{\mathrm{Pr}}A\left(\frac{\partial\theta}{\partial y}\right)^2-Q\theta-Df\frac{\partial}{\partial y}\left[(1+Dc\phi)\frac{\partial\phi}{\partial y}\right]=0, \tag{8}$$

$$\Delta_3\equiv\frac{\partial\psi}{\partial y}\frac{\partial\phi}{\partial x}-\frac{\partial\psi}{\partial x}\frac{\partial\phi}{\partial y}+\frac{\partial}{\partial x}[\ln(\Delta C)]-\frac{1}{Le}\frac{\partial}{\partial y}\left[(1+Dc\phi)\frac{\partial\phi}{\partial y}\right]+K\phi$$
$$-Sr(1+Dc\phi)\frac{\partial^2\theta}{\partial y^2}=0. \tag{9}$$

The boundary conditions in Eqn. (5) become:

$$\frac{\partial\psi}{\partial y}=x+a\frac{\partial^2\psi}{\partial y^2},\ \frac{\partial\psi}{\partial x}=0,\ \phi=1,\ \theta=1+b\frac{\partial\theta}{\partial y}\ \text{ at }\ y=0,$$
$$\frac{\partial\psi}{\partial y}\to S\,x,\ \theta\to 0,\ \phi\to 0\quad\text{as}\quad y\to\infty. \tag{10}$$

The controlling parameters are: Dufour ($D_f = D_\infty K_T\Delta C/C_sC_p\alpha_m\Delta T$), Soret ($S_r = D_\infty K_T\Delta T/T_m\alpha_m\Delta C$), magnetic field ($M = \sigma B^2{}_0/\rho_\infty c$), radiation ($R=3k_1k_\infty/16\sigma_1T^3{}_\infty$), generation/absorption ($Q=Q_0/c\,\rho_\infty c_\mathrm{p}$), porosity ($\Omega=\nu/c\,K_0$), velocity slip ($a=\sqrt{c\nu_\infty}\ N_1$), thermal slip ($b=\sqrt{c/\nu_\infty}\ D_1$), stretching ($S=a_1/c$), chemical reaction ($K=k_0/c$), Prandtl number ($\mathrm{Pr}=\mu_\infty c_\mathrm{p}/k_\infty$), Lewis number ($Le=\nu_\infty/D_\infty$). The wall temperature and concentration varied nonlinearly as $Tw=T_\infty + c_3x^n$ and $C_w = C_\infty + c_4x^n$, where C_3, C_4 are constants and n is the power law index.

SYMMETRY ANALYSIS

In this section, we shall show how scaling group transformation (special form of Lie group) transforms the governing equations into similarity equations. We begin our analysis by selecting the following scaling group of transformation (Seshadri & Na, 1985; Uddin *et al*., 2012),

$$\Gamma: x^* = xe^{\varepsilon\alpha_1}, y^* = ye^{\varepsilon\alpha_2}, \psi^* = \psi e^{\varepsilon\alpha_3}, \theta^* = \theta e^{\varepsilon\alpha_4}, \quad \phi^* = \phi e^{\varepsilon\alpha_5}, \beta_T^* = \beta_T e^{\varepsilon\alpha_6}, \beta_C^* = \beta_C e^{\varepsilon\alpha_7}. \tag{11}$$

Here ε ($\neq 0$) is a parameter and α_i (i = 1,2,3,...,7) are all arbitrary, real constants not all-zero simultaneously. Transformations in Eqn. (11) may be treated as a point transformation transforming the coordinates:

$$(x, y, \psi, u_e, \theta, \phi, \beta_T, \beta_C) \text{ to } (x^*, y^*, \psi^*, u_e^*, \theta^*, \phi^*, \beta_T^*, \beta_C^*).$$

We now investigate the relationship among the exponents $\alpha's$ such that:

$$\Delta_j\left(x^*, y^*, , u^*, v^* \cdots, \frac{\partial^3 \psi^*}{\partial y^{*3}}\right) = H_j\left(x, y, u, v, \cdots, \frac{\partial^3 \psi}{\partial y^3}; a\right)\Delta_j\left(x, y, \cdots, \frac{\partial^3 \psi}{\partial y^3}\right), (j = 1,2,3)$$

since this is the requirement for the differential forms Δ_1, Δ_2 and Δ_3 to be conformally invariant under the transformation group (11). Substituting the transformations (11) in Eqns. (14)-(16), we have:

$$\begin{aligned}
&\Delta_1 \equiv \frac{\partial \psi^*}{\partial y^*}\frac{\partial^2 \psi^*}{\partial x^* \partial y^*} - \frac{\partial \psi^*}{\partial x^*}\frac{\partial^2 \psi^*}{\partial y^{*2}} + \alpha_0 e^{-\alpha_0 \theta^*}\frac{\partial \theta^*}{\partial y^*}\frac{\partial^2 \psi^*}{\partial y^{*2}} - e^{-\alpha_0 \theta^*}\frac{\partial^3 \psi^*}{\partial y^{*3}} \\
&-u_e^*\frac{du_e^*}{dx^*} - (\Omega + M)\frac{\partial \psi^*}{\partial y^*} + (\Omega + M)u_e^* - \frac{g\,\Delta T}{c\sqrt{c\nu_\infty}}\beta_T^*\theta^* - \frac{g\,\beta_C\,\Delta C}{c\sqrt{c\nu_\infty}}\beta_C^*\phi \\
&= e^{\varepsilon(2\alpha_3 - \alpha_1 - 2\alpha_2)}\left[\frac{\partial \psi}{\partial y}\frac{\partial^2 \psi}{\partial x \partial y} - \frac{\partial \psi}{\partial x}\frac{\partial^2 \psi}{\partial y^2}\right] \\
&+ e^{\varepsilon(\alpha_4 + \alpha_3 - 3\alpha_1)}\alpha_0 e^{-\alpha_0 e^{\alpha_4}\theta}\frac{\partial \theta}{\partial y}\frac{\partial^2 \psi}{\partial y^2} - e^{\varepsilon(\alpha_3 - 3\alpha_1)}e^{-\alpha_0 e^{\alpha_4}\theta}\frac{\partial^3 \psi}{\partial y^3} \\
&-e^{\varepsilon\alpha_1}u_e\frac{du_e}{dx} - (\Omega + M)e^{\varepsilon(\alpha_3 - \alpha_2)}\frac{\partial \psi^*}{\partial y^*} + (\Omega + M)e^{\varepsilon\alpha_1}u_e \\
&-\frac{g\,\Delta T}{c\sqrt{c\nu_\infty}}e^{\varepsilon(\alpha_4 + \alpha_6)}\beta_T\theta - e^{\varepsilon(\alpha_5 + \alpha_7)}\frac{g\,\beta_C\,\Delta C}{c\sqrt{c\nu_\infty}}\beta_C\phi,
\end{aligned} \tag{12}$$

$$\Delta_2 \equiv \frac{\partial \psi^*}{\partial y^*}\frac{\partial \theta^*}{\partial x^*} - \frac{\partial \psi^*}{\partial x^*}\frac{\partial \theta^*}{\partial y^*} + \frac{\partial \psi^*}{\partial y^*}\theta^* \frac{\partial}{\partial x^*}\left[\ln(\Delta T)\right]$$
$$-\frac{1}{\mathrm{Pr}}\left[\frac{R+1+A\theta^*}{R}\right]\frac{\partial^2 \theta^*}{\partial y^{*2}} - \frac{1}{\mathrm{Pr}}A\left(\frac{\partial \theta^*}{\partial y^*}\right)^2 - Q\theta^* - Df\frac{\partial}{\partial y^*}\left[(1+Dc\,\phi^*)\frac{\partial \phi^*}{\partial y^*}\right] =$$
$$e^{\varepsilon(\alpha_3+\alpha_4-\alpha_1-\alpha_2)}\left[\frac{\partial \psi}{\partial y}\frac{\partial \theta}{\partial x} - \frac{\partial \psi}{\partial x}\frac{\partial \theta}{\partial y} + \frac{\partial \psi}{\partial y}\theta\frac{\partial}{\partial x}\left[\ln(\Delta T)\right]\right]$$
$$-\frac{1}{\mathrm{Pr}}e^{\varepsilon(\alpha_4-2\alpha_2)}\left[\frac{R+1+e^{\varepsilon\alpha_4}A\theta}{R}\right]\frac{\partial^2 \theta}{\partial y^2} - \frac{1}{\mathrm{Pr}}A\,e^{\varepsilon(2\alpha_4-2\alpha_2)}\left(\frac{\partial \theta}{\partial y}\right)^2$$
$$-Qe^{\varepsilon\alpha_4}\theta - Dfe^{\varepsilon(\alpha_5-2\alpha_2)}(1+Dc\,e^{\varepsilon\alpha_5}\phi)\frac{\partial^2 \phi}{\partial y^2} - Df\,Dce^{\varepsilon(2\alpha_5-2\alpha_2)}\left(\frac{\partial \phi}{\partial y}\right)^2 \quad (13)$$

$$\Delta_3 \equiv \frac{\partial \psi^*}{\partial y^*}\frac{\partial \phi^*}{\partial x^*} - \frac{\partial \psi^*}{\partial x^*}\frac{\partial \phi^*}{\partial y^*} + \frac{\partial}{\partial x^*}\left[\ln(\Delta C)\right] - \frac{1}{Le}\frac{\partial}{\partial y^*}\left[(1+Dc\,\phi^*)\frac{\partial \phi^*}{\partial y^*}\right]$$
$$+K\,\phi^* - Sr(1+Dc\,\phi)\frac{\partial^2 \theta}{\partial y^2} = e^{\varepsilon(\alpha_3+\alpha_5-\alpha_1-\alpha_2)}\left[\frac{\partial \psi}{\partial y}\frac{\partial \phi}{\partial x} - \frac{\partial \psi}{\partial x}\frac{\partial \phi}{\partial y} + \frac{\partial}{\partial x}\left[\ln(\Delta C)\right]\right]$$
$$-\frac{1}{Le}\left[1+Dc\,e^{\varepsilon\alpha_5}\phi\right]e^{\varepsilon(\alpha_5-2\alpha_2)}\frac{\partial^2 \phi}{\partial y^2} - \frac{Dc}{Le}e^{\varepsilon(\alpha_5-2\alpha_2)}\left(\frac{\partial \phi}{\partial y}\right)^2 \quad (14)$$
$$-Sr\left[1+Dc\,e^{\varepsilon\alpha_5}\phi\right]e^{\varepsilon(\alpha_4-2\alpha_2)}\frac{\partial^2 \theta}{\partial y^2}.$$

The system remains invariant under the group transformation Γ if the exponent satisfies the following relationship:

$$\alpha_2 = \alpha_4 = \alpha_5 = 0,\ \alpha_1 = \alpha_3 = \alpha_6 = \alpha_7. \quad (15)$$

The set of transformations (11) reduces to:

$$x^* = xe^{\varepsilon\alpha_1}, y^* = y, \psi^* = \psi e^{\varepsilon\alpha_1}, \theta^* = \theta, \phi^* = \phi, \beta_T^* = \beta_T e^{\varepsilon\alpha_1}, \beta_C^* = \beta_C e^{\varepsilon\alpha_1}. \quad (16)$$

Using Taylor series expansion in powers of $\mathcal{E}$, keeping the terms up to the first degree and neglecting higher powers of $\mathcal{E}$, we have:

$$x^* - x = \varepsilon\alpha_1 x, y^* - y = 0, \psi^* - \psi = \varepsilon\alpha_1\psi, \theta^* - \theta = \phi^* - \phi = 0,$$
$$\beta_T^* - \beta_T = \varepsilon\alpha_1\beta_T, \beta_C^* - \beta_C = \varepsilon\alpha_1\beta_C. \quad (17)$$

SIMILARITY TRANSFORMATIONS

It is clear that $y^* = y, \theta^* = \theta, \phi^* = \phi$ are invariant. Let us define them by

$$\eta = y,\ \theta = \theta(\eta),\ \phi = \phi(\eta). \tag{18}$$

The other invariants can be found by solving the following characteristic equations:

$$\frac{dx}{\alpha_1 x} = \frac{d\psi}{\alpha_1 \psi} = \frac{d\beta_T}{\alpha_1 \beta_T} = \frac{d\beta_C}{\alpha_1 \beta_C}. \tag{19}$$

Solving (18), we get the following absolute invariants (similarity transformations):

$$\psi = x f(\eta),\ \beta_T = \beta_{T_0} x,\ \beta_C = \beta_{C_0} x. \tag{20}$$

Here β_{T_0} and β_{C_0} are constant thermal and mass expansion coefficients, η is the similarity independent variable and $f(\eta)$ is the dimensionless stream function.ηf

SIMILARITY EQUATIONS

With the use of the definitions in Eqns. (18) and (20), Eqns. (7)-(10) reduce to the following similarity equations:

$$f''' - \alpha_0 f''\theta' + e^{\alpha_0 \theta}\left[ff'' - f'^2 + S^2 - (\Omega + M)(f' - S) + Gr\theta + Gc\phi \right] = 0,$$

$$\left[\frac{R + 1 + A\theta}{\Pr R}\right]\theta'' + A\theta'^2 + f\theta' - n f'\theta + Q\theta + Df\left(1 + Dc\phi\right)\phi'' + Df\, Dc\,\phi'^2 = 0, \tag{21}$$

$$(1 + Dc\phi)\phi'' + Dc\,\phi'^2 + Le\left[f\phi' - n f'\phi - K\phi + Sr(1 + Dc\phi)\theta'' \right] = 0. \tag{22}$$

The boundary conditions (10) yield:

$$\begin{aligned} &f(0) = 0,\ f'(0) = 1 + af''(0),\ \theta(0) = 1 + b\theta'(0),\ \phi(0) = 1, \\ &f'(\infty) - S = \theta(\infty) = \phi(\infty) = 0. \end{aligned} \tag{23}$$

Here $Gr = g\beta_{T_0} L\Delta T / c\sqrt{c\nu_\infty}$, $Gc = g\,\beta_{C_0} L\Delta C / c\sqrt{c\nu_\infty}$ are thermal and mass Grashof numbers respectively.

It is interesting to note that in the case of no-slip boundary conditions ($a = b = 0$) and in the case of the constant thermal conductivity and mass diffusivity ($A = Dc = 0$) we can recover the similarity solution reported by Abdel-Rahman (2010).

QUANTITIES OF ENGINEERING INTEREST

The quantities of interest are the friction factor $C_{f\bar{x}}$, local Nusselt number $Nu_{\bar{x}}$ and the local Sherwood number $Sh_{\bar{x}}$ respectively. These quantities can be conveniently calculated from the following relations:

$$C_{f\bar{x}} = \frac{\mu}{\rho \bar{u}_w^2}\left(\frac{\partial \bar{u}}{\partial \bar{y}}\right)_{\bar{y}=0}, Nu_{\bar{x}} = \frac{-\bar{x}}{T_w - T_\infty}\left(\frac{\partial T}{\partial \bar{y}}\right)_{\bar{y}=0}, Sh_{\bar{x}} = \frac{-\bar{x}}{C_w - C_\infty}\left(\frac{\partial C}{\partial \bar{y}}\right)_{\bar{y}=0}. \quad (24)$$

Substituting Eqns. (6), (18) and (20) into Eqn. (24), the physical quantities can be written as:

$$\sqrt{\mathrm{Re}_{\bar{x}}}\, C_{f\bar{x}} = \left[1 + A(1-\theta(0)\right] f''(0), \frac{Nu_{\bar{x}}}{\sqrt{\mathrm{Re}_{\bar{x}}}} = -\theta'(0), \frac{Sh_{\bar{x}}}{\sqrt{\mathrm{Re}_{\bar{x}}}} = -\phi'(0), \quad (25)$$

where $\mathrm{Re}_{\bar{x}} = \frac{u_w \bar{x}}{\nu}$ is the local Reynolds number.

RESULTS AND DISCUSSION

The similarity Eqns. (20)-(22) with boundary conditions in Eqn. (23) were solved numerically using the Runge-Kutta-Fehlberg fourth-fifth order numerical method in Maple 13 (White & Subramanian, 2010). The details of the method were described in a recent paper by Uddin *et al*. (2013). The effect of the controlling parameters on the dimensionless velocity, temperature, concentration, friction factor, heat transfer and mass transfer rates were investigated and presented in graphs. In the case of constant viscosity $\alpha_0 = 0$, constant thermal conductivity A = 0 and constant mass diffusivity (Dc = 0), the results of the skin friction factor, the rate of heat and mass transfer were compared with the published results for some special cases. The comparisons are given in Tables 1-3 and were found to have a good agreement.

Fig.2 illustrates the effect of the porosity and viscosity parameters on the diemsionless velocity. It was noticed that both the parameters reduced the dimensionless velocity. The numerical computations for these graphs were performed for and , which corresponded to assisting mixed convective flow. This (assisting flow) happens in many engineering applications such as cooling of electronic components and nuclear reactors. Fig.3 shows the influence of the radiation and thermal conductivity parameters on the dimensionless temperature. The dimensionless temperature decreased with the radiation parameter. It was further found that temperature increased with the increase in the thermal conductivity parameter. Physically increasing thermal diffusivity parameter means the increasing of the thermal conductivity of the fluid. Increasing thermal conductivity implies an increase in temperature. The effect of the thermal slip and heat generation parameters on the dimensionless temperature is shown in Fig.4. It was noticed that the temperature reduced with the increase of the thermal slip parameter. We also noticed that due to the increasing value of the generation parameter, the temperature increased. This was because physically, heat generation ( ) in the fluid will enhance thermal energy to the flow and hence, for a positive , temperature will rise. The effect of the mass diffusivity and Dufour number on the dimensionless temperature is shown in Fig.5. We observed from Fig.5 that the temperature enhances with improvements in the mass diffusivity parameter.

TABLE 1: Comparison of the Heat and Mass Transfer Rates Under Soret and Dufour Effects for Different Q when $R = 0.4$, K=0.6, α_0 - $Gr = Gc = M = a = 6 = A = Dc = 0$, $S = Le = \Pr = n = \Omega = 1$

Q	Sr	Df	$\sqrt{\mathrm{Re}_{\bar{x}}}\,Nu_{\bar{x}}$			$\sqrt{\mathrm{Re}_{\bar{x}}}\,Sh_{\bar{x}}$		
			Tsai et al. (2009)	Abdel Rahman (2010)	Present results	Tsai et al. (2009)	Abdel Rahman (2010)	Present results
0.0	2.0	0.03	0.6641	0.6636	0.66405	1.0726	1.0724	1.07262
	1.0	0.12	0.6403	0.6401	0.64030	1.2858	1.2856	1.28579
	0.5	0.30	0.5881	0.5876	0.58806	1.3941	1.3939	1.39409
	0.1	0.60	0.4972	0.4966	0.49716	1.4589	1.4588	1.45897
0.5	2.0	0.03	0.5518	0.551	0.55178	1.2070	1.2070	1.20707
	1.0	0.12	0.5254	0.5238	0.52544	1.3545	1.3546	1.35453
	0.5	0.30	0.4695	0.4687	0.46947	1.4293	1.4292	1.42938
	0.1	0.60	0.3749	0.3740	0.37486	1.4661	1.4660	1.46613
-0.5	1.0	0.03	0.7619	0.7616	0.76188	0.9499	0.9497	0.94992
	1.0	0.12	0.7403	0.740	0.74029	1.2231	1.2230	1.22313
	0.5	0.30	0.6911	0.6907	0.69107	1.3620	1.3618	1.36198
	0.1	0.60	0.603	0.6027	0.60303	1.4524	1.4523	1.45247

TABLE 2: Comparison of the Skin Friction, the Heat and Mass Transfer Rates for Different Values of M when $R = 0.4$, $K = 0.6$, $S = 0.5$, $Df = 0.12$, $\Pr = n = Le = 1$, α_0 = Gr=Gc=Ω=a=b=A=Dc=0

M	$\sqrt{\mathrm{Re}_{\bar{x}}}\,C_{f\bar{x}}$		$\sqrt{\mathrm{Re}_{\bar{x}}}\,Nu_{\bar{x}}$		$\sqrt{\mathrm{Re}_{\bar{x}}}\,Sh_{\bar{x}}$	
	Abdel Rahman (2010)	Present results	Abdel Rahman (2010)	Present results	Abdel Rahman (2010)	Present Results
1	0.8321	0.832126	0.5267	0.526593	1.2001	1.200041
3	1.0910	1.091021	0.5144	0.514332	1.1856	1.185622
5	1.2998	1.299798	0.5069	0.506775	1.1759	1.175899

TABLE 3 : Comparison of the Skin Friction, the Heat and Mass Transfer Rates for different Values of S when K= 0.6, R = 0.4, Df = 0.12, $\Pr = n = Le = Sr = 1$, α_0 = Gr =Gc = A = Dc =Ω = a = b = 0

S	$\sqrt{\mathrm{Re}_{\bar{x}}}\,C_{f\bar{x}}$			$\sqrt{\mathrm{Re}_{\bar{x}}}\,Nu_{\bar{x}}$			$\sqrt{\mathrm{Re}_{\bar{x}}}\,Sh_{\bar{x}}$		
	Tsai et al. (2009)	Abdel Rahman (2010)	Present	Tsai et al. (2009)	Abdel Rahman (2010)	Present	Tsai et al. (2009)	Abdel Rahman (2010)	Present
0.5	-0.6673	-0.6673	-0.6673	0.5368	0.5368	0.5367	1.2109	1.2109	1.2109
1.0	0	0.0132	0.0000	0.6403	0.6359	0.6403	1.2858	1.2835	1.2857
1.5	0.9095	0.8989	0.9095	0.7282	0.7258	0.7282	1.3653	1.3638	1.3653

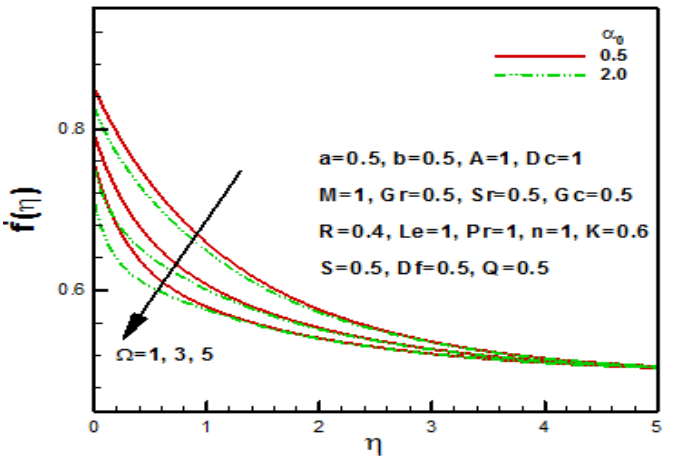

Fig.2: Effect of the porosity and viscosity parameters on dimensionless velocity.

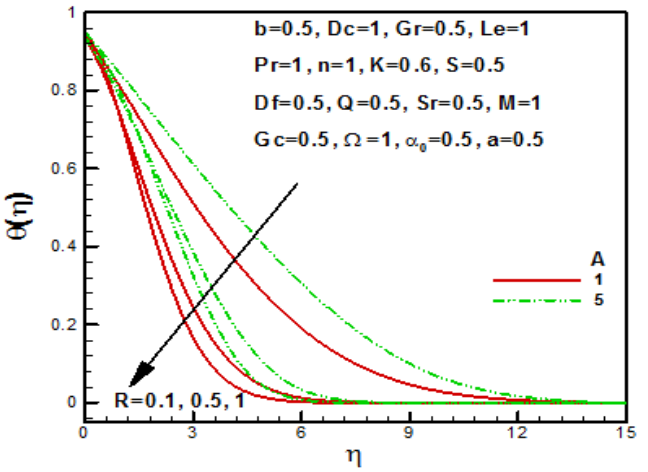

Fig.3: Effect of the radiation and thermal conductivity parameters on dimensionless temperature.

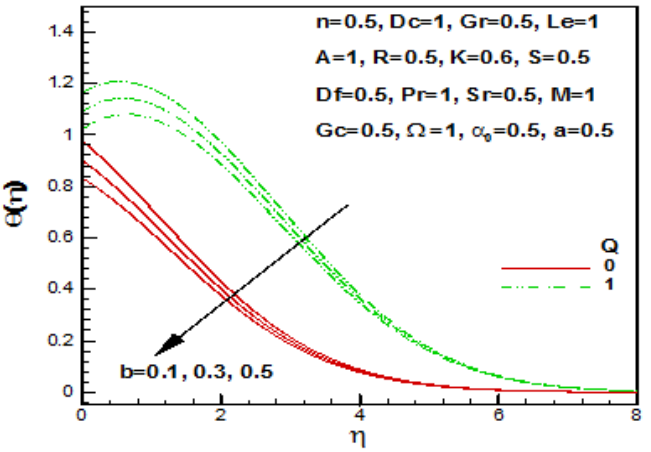

Fig.4: Effect of thermal slip and heat generation parameters on dimensionless temperature.

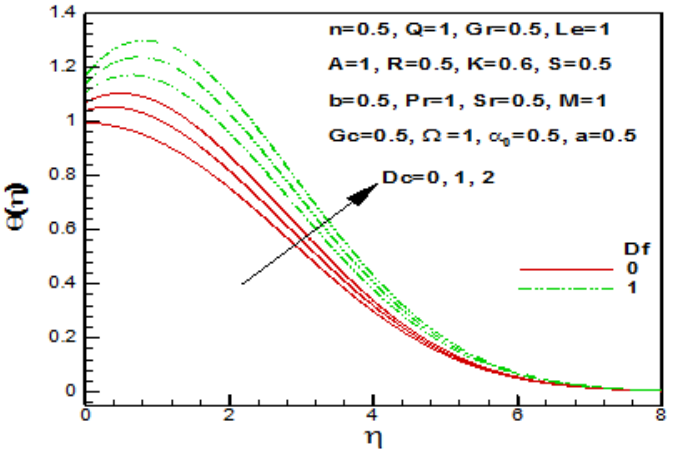

Fig.5: Effect of the Dufour and concentration diffusivity parameters on dimensionless temperature.

Fig.6 shows that the dimensionless concentration increased as the mass diffusivity parameter increased. This was due to the fact that an increase in the mass diffusivity parameter caused an increase in the mass diffusivity, which is a linear function of concentration. As a result, increasing mass diffusivity increased the concentration. This important finding was overlooked by all of the previous authors. Concentration variations due to Lewis number and Soret number are shown in Fig.7. It was observed that concentration as well as the concentration boundary layer thickness was increased as the Lewis number increases.

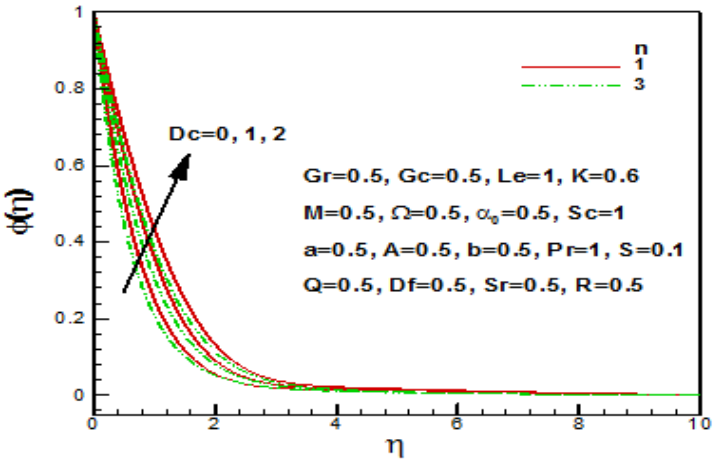

Fig.6: Effect of concentration diffusivity and power-law index parameters on dimensionless concentration.

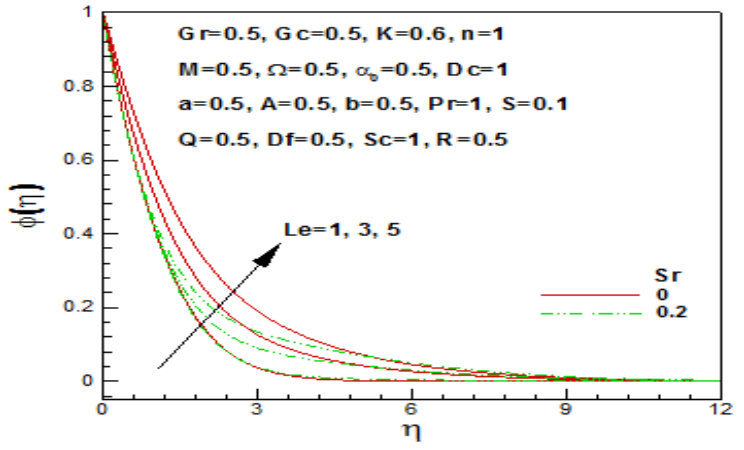

Fig.7: Effect of the Schmidt number and Soret number on dimensionless concentration.

The effect of different parameters on skin friction is illustrated in Fig.8 and Fig.9. It was observed from Fig.8 that skin friction was a decreasing function of the velocity slip parameter and the thermal and concentration Grashof number. This was due to the fact that in the presence of a magnetic field, the slip parameter increased the velocity at the surface, which reduced the friction. In this case, it was assumed that the viscosity was constant. Also, the decrease in the wall temperature and concentration decreased the thermal and concentration Grashof numbers, which helped in reducing the skin friction. The variation of the skin friction with magnetic field for different values of stretching and porosity parameters is illustrated in Fig.9. It was clear that the skin friction increased with an increase in the magnetic and porosity parameters. This was due to the fact that the magnetic field decreased the velocity at the surface, which increased the skin friction. Similarly, the increase in the porosity parameter reduced the velocity at the surface and as a result, the skin friction increased. It is important to note that the stretching of the plate increased the velocity and hence, decreased the skin friction.

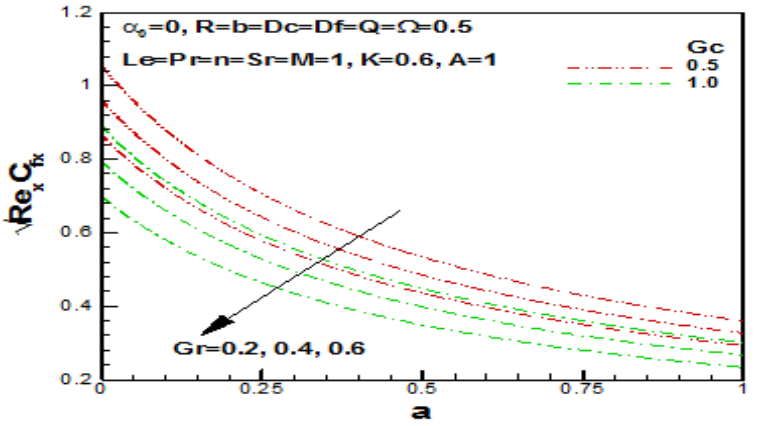

Fig.8: Effect of slip parameter and thermal and concentration Grashof numbers on skin friction.

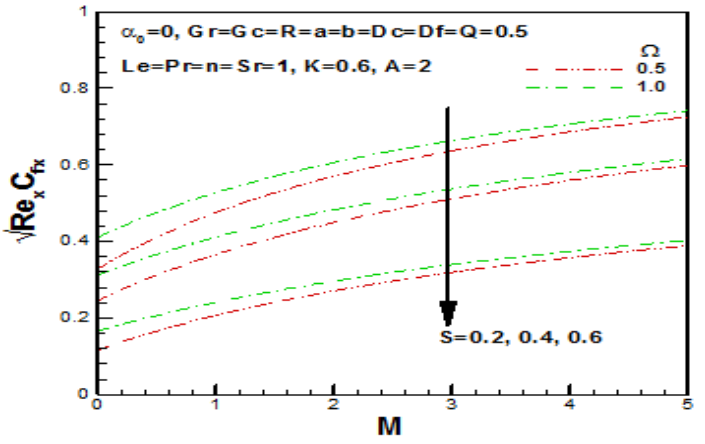

Fig.9: Effect of the magnetic, stretching and porosity parameters on skin friction.

The variation of the dimensionless heat transfer rates versus different parameters is depicted in Fig.10-12. Fig.10 reveals that the dimensionless heat transfer rate was a weak function of Soret and Dufour numbers. It was found that the dimensionless heat transfer rates decreased with an increase in the heat generation parameter. The variation of the dimensionless heat transfer rates versus the stretching parameter for different values of the power-law index and chemical reaction parameter is shown in Fig.11. Observe that the rate of heat transfer increased due to increases in the stretching, power-law index and chemical reaction parameters. The variation of the dimensionless heat transfer rates versus magnetic parameters for different values of the velocity slip and viscosity parameters is illustrated in Fig.12. We may see in Fugure 12 that the heat transfer rate increased for increasing values of slip and viscosity parameter whilst it decreased with increasing values of the magnetic field parameter.

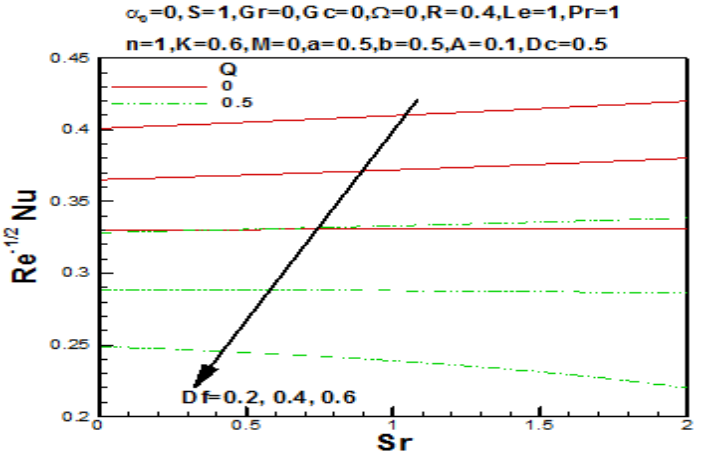

Fig.10: Variation of the dimensionless heat transfer rates versus Soret numbers for different Dufour numbers and heat generation parameters.

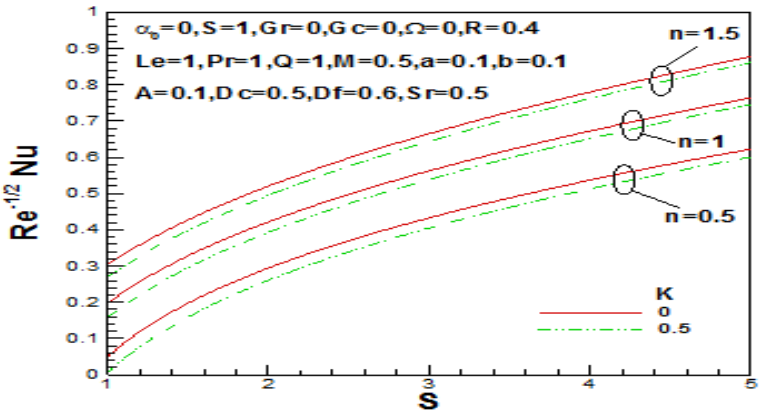

Fig.11: Variation of the dimensionless heat transfer rates versus stretching parameter for different power-law index and chemical reaction parameters.

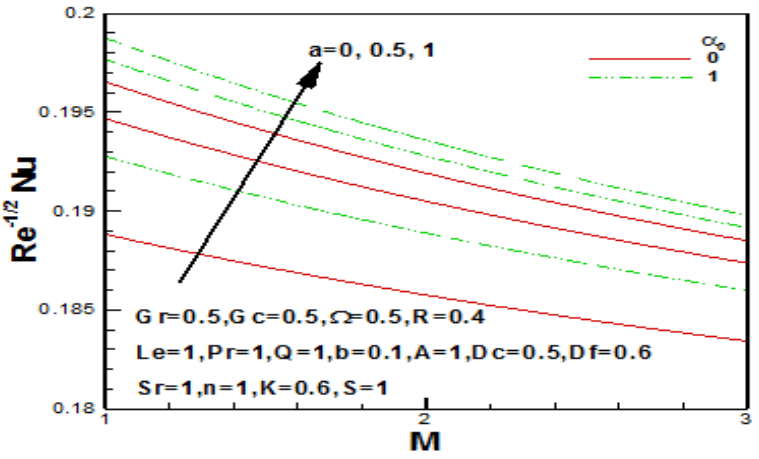

Fig.12: Variation of the dimensionless heat transfer rates versus magnetic parameter for different velocity slip and viscosity parameters.

The variation of the dimensionless mass transfer rates versus different parameters is depicted in Fig.13-15. Fig.13 exhibits that the rate of mass transfer rose with the rise in heat generation and the Dufour numbers but decreased as the value of the Soret number declined. It is important to note that in the absence of heat generation, dimensionless mass transfer rates decreased for small Dufour numbers and become almost constant for large Dufour numbers. But as heat generation increased, the dimensionless mass transfer rates started increasing with the increase in both Soret and Dufour numbers. We noticed from Fig.14 that the dimensionless mass transfer rates increased with the stretching parameter, power-law index and chemical reaction parameters. The variation of dimensionless mass transfer rates versus magnetic parameter for different values of velocity slip and viscosity parameters is shown in Fig.15. It was found that the mass transfer rate increased with the velocity slip and viscosity parameters.

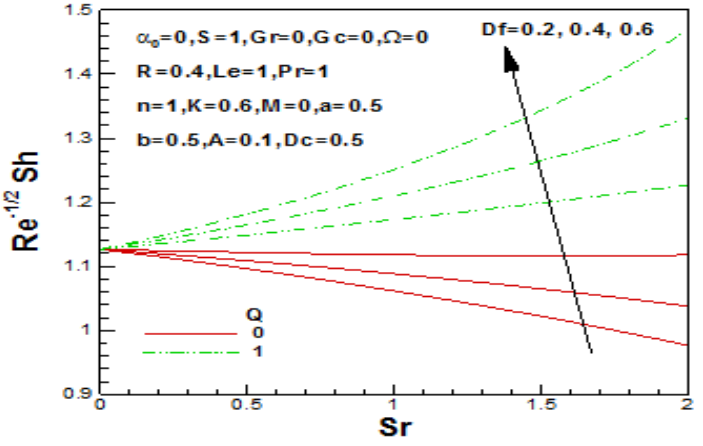

Fig.13: Variation of the dimensionless mass transfer rates versus Soret numbers for different Dufour numbers and heat generation parameters.

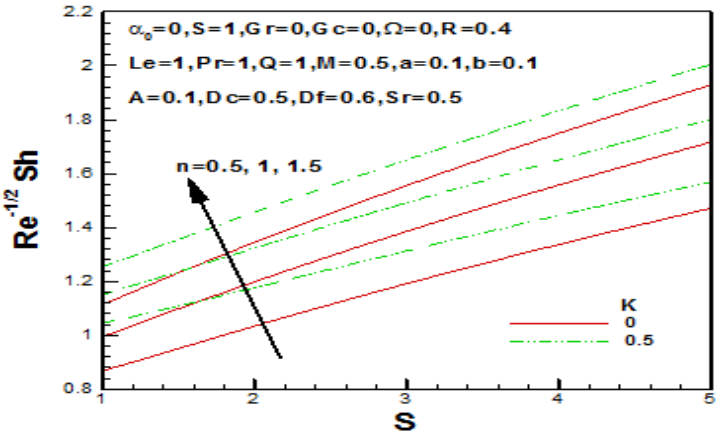

Fig.14: Variation of the dimensionless mass transfer rates versus stretching parameter for different power-law index and chemical reaction parameters.

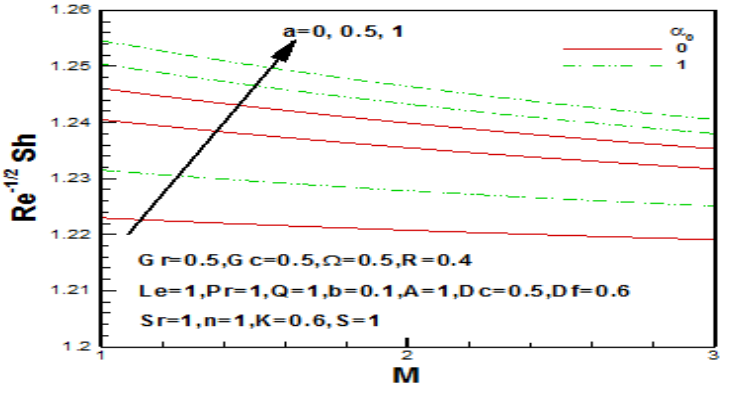

Fig.15: Variation of the dimensionless mass transfer rates versus magnetic parameter for different velocity slip and viscosity parameters.

CONCLUSION

The steady laminar boundary layer slip flow of a viscous incompressible Newtonian fluid along a moving stretching sheet immersed in a porous medium was studied numerically. The temperature- dependent viscosity and thermal conductivity and concentration-dependent mass diffusivity were taken into account. By using a scaling group transformation, the transport equations along with the boundary conditions were converted to similarity equations. From our analysis, we concluded that for some types of mixture (for example, H2-air) with the light and medium molecular weight, the magnetic field and the Soret and Dufour's effects with the variable mass diffusivity play an important role and should be taken into consideration as well.

REFERENCES

Abdel-Rahman, G. M. (2010). Thermal-diffusion and MHD for Soret and Dufour's effects on Hiemenz flow and mass transfer of fluid flow through porous medium onto a stretching surface. *Physica B, 405*, 2560-2569.

Aziz, A. (2010). Hydrodynamic and thermal slip flow boundary layers over a flat plate with constant heat flux boundary condition. *Communication in Nonlinear Science and Numerical Simulation, 15*, 573-580.

Crane, L. J. (1970). Flow past a stretching plate. *Zeitschrift für angewandte Mathematik und Physik ZAMP, 21*, 645-647.

Eckert, E. R., & Drake, R. M. (1972). *Analysis of heat and mass transfer.* New York: McGraw Hill.

Gifford, W. A. (2004). The effect of wall slip on the performance of flat extrusion dies. *Polymer Engineering. & Science, 41*, 1886-1892.

Hayat, T., Mustafa, M., & Pop, I. (2010). Heat and mass transfer for Soret and Dufour's effect on mixed convection boundary layer flow over a stretching vertical surface in a porous medium filled with a viscoelastic fluid. *Communication in Nonlinear Science and Numerical Simulation, 15,* 183-1196.

Ireland, P. M., & Jameson, G. J. (2009). Foam slip on surfaces of intermediate or low wettability. *Chemical Engineering Science, 64*, 3859-3867.

Ishak, A., Nazar, R., & Pop, I. (2009). Boundary layer flow and heat transfer over an unsteady stretching vertical surface. *Mecanica, 44,* 369-375.

Jiji, L. M. (2009). *Heat convection.* (2nd ed., Chapter 11). Springer, New York.

Khaled, A. R. A., & Vafai, K. (2004). Analysis of oscillatory flow disturbances and thermal characteristics inside fluidic cells due to fluid leakage and wall slip conditions. *Journal of Biomechanics, 37,* 721-729.

Lahjomri, J., & Oubarra A. (2013). Hydrodynamic and thermal characteristics of laminar slip flow over a horizontal isothermal flat plate. *ASME Journal of Heat Transfer, 135*(2), 021704.

Mansour, M. A., & El-Anssary, N. F., & Aly, A. M. (2008). Effects of chemical reaction and thermal stratification on MHD free convective heat and mass transfer over a vertical stretching surface embedded in porous media considering Soret and Dufour numbers. *Chemical Engineering Journal,145*, 340-345.

Nield, D. A., & Bejan, A. (2013). *Convection in porous media.* (4th ed.). New York: Springer.

Noghrehabadi, A., Pourrajab, R., & Ghalambaz, M. (2012). Effect of partial slip boundary condition on the flow and heat transfer of nanofluids past stretching sheet prescribed constant wall temperature. *International Journal of Thermal Sciences, 54,* 253-261.

Postelnicu, A. (2010). Heat and mass transfer by natural convection at a stagnation point in a porous medium considering Soret and Dufour effects. *Heat Mass Transfer, 46,* 831-840.

Seddeek, M. A. & Salem, A. M. (2005). Laminar mixed convection adjacent to vertical continuously stretching sheets with variable viscosity and variable thermal diffusivity. *Heat Mass Transfer, 41*, 1048-1055.

Seshadri R., & Na T. Y. (1985). *Group invariance in engineering boundary value problems*. Springer, New York, USA.

Tsai, R., & Huang, J. S. (2009). Heat and mass transfer for Soret and Dufour's effects on Hiemenz flow through porous medium onto a stretching surface. *International Journal of Heat Mass Transfer, 52*(9), 2399-2406.

Uddin, M. J., Ferdows, M., Be´g, O. A. (2013). Group analysis and numerical computation of magneto-convective non-Newtonian nanofluid slip flow from a permeable stretching sheet, *Applied Nanoscience, 4*(7), 897-910.

Uddin, M. J., Khan, W. A., & Ismail, A. I. M. (2012). Scaling group transformation for MHD boundary layer slip flow of a nanofluid over a convectively heated stretching sheet with heat generation. *Mathematical Problems in Engineering, 2012*, Article ID 934964, 20 pp.

Vajravelu, K., Prasad, K. V., Lee, J., Lee, C., Pop, I., Robert, A., & Van Gorder. (2011). Convective heat transfer in the flow of viscous Ag–water and Cu–water nanofluids over a stretching surface. *International Journal of Thermal Sciences, 50*(5), 843-851.

White, R. E., & Subramanian, V. R. (2010). *Computational methods in chemical engineering with maple*. New York: Springer